AIChE

A Dynamic Analysis of Chalcopyrite Bioleaching in Continuous Flow Reactor Systems

Athanasios Kotsiopoulos, Geoffrey S. Hansford, and Randhir Rawatlal
Dept. of Chemical Engineering, University of Cape Town, Rondebosch 7701, South Africa

DOI 10.1002/aic.12753
Published online September 23, 2011 in Wiley Online Library (wileyonlinelibrary.com).

A dynamic analysis of chalcopyrite bioleaching was performed in continuous flow systems. In contrast to a previous batch analysis[1] in which the influence of particle surface area on reaction rate was not accounted for, the unsteady-state change in particle surface area was integrated into the dynamic analysis by application of the modified PBM.[2] The current study extends the analysis to include the influence of convective flow on the system. It is demonstrated that the analysis can be used to determine feasible control strategies for operating near the steady-state maximum rate that is stable. Two strategies were evaluated for the purpose of increasing the leaching rates, showing that an increased rate of 56% is feasible. Analysis on experimental data showed that increased rates can be achieved by controlling the biomass concentration and ferric:ferrous ion ratio at an optimum by increasing the solids loading [m/v] in the reactor. © 2011 American Institute of Chemical Engineers *AIChE J,* 58: 2428–2440, 2012
Keywords: reaction kinetics, reactor analysis, mathematical modeling

Introduction

Industrial bioleaching processes have been developed for heap or tank reactor systems. In heap leaching, constructed mounds of crushed ore are irrigated at the top of the heap with an acidic leach solution. The mineral rich leachate is then recovered for further downstream processing.[3] In tank bioleaching, the extraction of metals from sulfide minerals is often performed in a series of aerated stirred-tank reactors.[3] In contrast to heap leaching, the primary operating variables, namely temperature, pH, oxygen and carbon dioxide transfer, can effectively be controlled to obtain a higher degree of extraction.[4,5]

In the bioleaching process, mineral dissolution occurs when ferric ions attack the metal sulfide particles at the surface releasing ferrous ions in a proton rich solution (Eq. 1). Ferric ions are regenerated by the oxidation of ferrous ions (Eq. 2). The recovery of metals is accelerated by the metabolic activity of iron and sulfur oxidizing microbes maintaining an environment that promotes the liberation of ferrous ions from the mineral sulfide particles

$$CuFeS_2 + 4Fe^{3+} \rightarrow Cu^{2+} + 5Fe^{2+} + 2S^0 \quad (1)$$

$$4Fe^{2+} + O_2 + 4H^+ \rightarrow 4Fe^{3+} + 2H_2O \quad (2)$$

The constant release of ferrous ions from the particle surface into solution results in the particle surface area or size diminishing with reaction. The variation in particle size in the reactor causes variable reactivities (from particle to particle) to occur. When developing a reactor model, one method of keeping track of these surface area changes and their resulting influence on the reaction rate is the population balance model (PBM). PBMs are often applied in particulate processes and have been successfully applied in tank bioleaching.[6]

In a previous study, a model was developed to determine the reactor performance of continuous flow bioleach reactors.[2] The objective of the study was to develop a reactor model for tank bioleaching using a modified population balance model (PBM) approach that incorporated the bioleaching subprocess mechanism for both mineral and aqueous phases (Eqs. 1 and 2). Previously published reactor models[5–11] was formulated under the assumption that the bioleaching process is at steady state and is perfectly mixed. Since the residence time distribution (RTD) appears explicitly in the novel formulation, and given that the unsteady-state RTD[12] and imperfect mixing theory have recently become available, it was possible to extend the reactor model to unsteady state behavior and imperfect mixing.[2]

The reactor model presented by Kotsiopoulos et al.[2] applied a PBM using a segregation approach which monitors the change in the particle properties based on the particle residence time and inlet size. This approach requires the solution of a system of ordinary differential equations using well-defined initial conditions rather than the computationally expensive partial differential equations usually associated with traditional PBMs.

Model verification was facilitated by published data from the Fairview mine in South Africa.[13] Simulation results indicated that the model was in good agreement with the data.[2] The model was formulated in a generic form to allow for a range of mineral sulfide ores to be investigated and to determine their resultant influence on the overall reactor performance.

Correspondence concerning this article should be addressed to R. Rawatlal at randhir.rawatlal@uct.ac.za.

In this study, the unsteady-state analogue to the segregation approach outlined in Kotsiopoulos et al.[2] will be developed. Since the PBM incorporates nonlinear intrinsic rate expressions, a dynamic analysis of the bioleaching of mineral sulfide ores was necessary to ascertain whether more than one steady state may exist in batch and continuous flow bioleach reactor systems. The dynamic analysis was initially developed assuming a fixed particle surface area during leaching to determine the influence of biomass concentration, the ferric:ferrous ion ratio and mean residence time on steady-state operation. Thereafter, by application of the modified PBM, the surface area assumption was relaxed to further establish the influence of time-varying particle surface area on observed steady states.

Reactor Model

To determine the overall performance of continuous flow bioleach reactors, the overall bioleaching rate is initially predicted. This is achieved by application of the PBM using a segregation approach developed by Kotsiopoulos et al.[2] The reactor model is briefly outlined in this section; comprehensive detail is available in Kotsiopoulos et al.[2]

The model was developed under the assumption that the inlet stream contains a nontrivial distribution in particle size, as well as a nontrivial distribution in particle residence time or age in the reactor. Since a nontrivial distribution in particle residence time exists, the reaction rate can be most easily be modeled using a segregation approach. By incorporating the age $I(\theta)$ and size $f_0(l_0)$ distributions, and defining $f_0(l_0)\Delta l_0$ and $I(\theta)\Delta\theta$ as the fraction of particles in the age range $[\theta, \theta + \Delta\theta]$ and size range $[l_0, l_0 + \Delta l_0]$ in the reactor, respectively, the overall reaction rate r^R [mol m^{-3} s^{-1}] in Eq. 3 was formulated using the segregation approach.

$$r^R = \int_0^\infty \int_0^\infty r'' A^p(\theta, l_0) \frac{M^p(\theta, l_0)}{V^R} \phi_{MS} N^T I(\theta) f_0(l_0) d\theta dl_0 \quad (3)$$

where A^P [m^2 kg^{-1}] is the particle specific surface area, M^P[kg] is the particle mass, V^R [m^3] is the volume of the reactor, ϕ_{MS} is the fraction of the mineral sulfide in the particles, and N^T is the total number of particles in the reactor.

Since the underlying kinetics in bioleaching systems is generally nonlinear, a rigorous dynamic analysis was undertaken to investigate any artifacts that may influence the reactor operation.[1,2] In the subsequent sections, the dynamic analysis for continuous flow reactor systems will be adapted from a batch system. For the sake of completeness, the dynamic analysis is initially introduced using a constant particle surface area assumption.

Batch Dynamics

The dynamics of chalcopyrite bioleaching was extensively studied for a range of solution redox potentials, biomass concentrations and temperature conditions in batch reactor systems.[1] It was established that the generally reported pseudo-steady state[10] (Eq. 4) for batch systems only holds for the ferrous ion

$$-r_{Fe^{2+}}^{\text{micro}} = -r_{Fe^{2+}}^{\text{chem}} \quad (4)$$

where $-r_{Fe^{2+}}^{\text{micro}}$ [mol m^{-3} s^{-1}] is the rate of microbial ferrous ion consumption, and $-r_{Fe^{2+}}^{\text{chem}}$ [mol m^{-3} s^{-1}] is the rate of chemical ferrous ion production.

It was proposed that since the combined concentration of ferric and ferrous ions are continuously changing with time and the only possible pseudo-steady state is at the point of equilibrium when the ferric:ferrous ion ratio R is constant or in pseudo-steady state with respect to the composition ratio, the rate of change in the ferric:ferrous ion ratio R can be evaluated by the dynamic expression derived in Eq. 5[1]

$$\frac{dR}{dt} = \frac{C_{Fe^{2+}} \cdot \frac{dC_{Fe^{3+}}}{dt} - C_{Fe^{3+}} \cdot \frac{dC_{Fe^{2+}}}{dt}}{C_{Fe^{2+}}^2} \quad (5)$$

where $\frac{dC_{Fe^{3+}}}{dt}$ and $\frac{dC_{Fe^{2+}}}{dt}$ are the material balances for the aqueous ferric and ferrous ions in the reactor, respectively, and R is the ratio of the concentration ferric ions relative to the concentration of ferrous ions.

The microbial oxidation rate $r_{Fe^{2+}}$ [mol m^{-3} s^{-1}] used in this study was developed by Hansford[14] (Eq. 6)

$$-r_{Fe^{2+}} \frac{C_x q_{Fe^{2+}}^{\max}}{1 + K\frac{C_{Fe^{3+}}}{C_{Fe^{2+}}}} \quad (6)$$

where $q_{Fe^{2+}}^{\max}$ [mol Fe^{2+} mol^{-1} carbon s^{-1}] is the maximum microbial specific ferrous iron utilization rate, K the inhibition constant, and C_X, $C_{Fe^{3+}}$, $C_{Fe^{2+}}$ are the concentrations of the biomass [mol carbon m^{-3}], ferric and ferrous ions [mol m^{-3}], respectively.

An empirical leaching rate expression developed by Petersen and Dixon[15] which imitates the proposed mechanism by Hiroyoshi et al.[16] and bioleaching trends observed by Kametani and Aoki[17] was used in the dynamic analysis of chalcopyrite bioleaching (Eq. 7). Unlike most mineral sulfide ores which increase monotonically with increasing ferric:ferrous ion ratio R, and, therefore, exhibit only a single steady state, chalcopyrite exhibited as many as three steady states. The empirical leaching rate expression proposed by Petersen and Dixon[15] which illustrates the nonmonotonic rate relationship of chalcopyrite with R is shown in Eq. 7

$$r_{cpy} = g_{py} \cdot f(X_{cpy}) \cdot R^{0.5} \left[A \cdot \exp\left(-\frac{R}{R_{\text{crit}}}\right) + B \cdot \left(1 - \exp\left(-\frac{R}{R_{\text{crit}}}\right)\right)\right] \quad (7)$$

where g_{py} is the mineral grade which is the fraction of mineral ore content in the ore body, $f(X_{cpy})$ the topological term which accounts for the change in the mineral reacting surface with particle conversion, A and B the temperature-dependent kinetic rate constants [mol m^{-2} s^{-1}], and R_{crit} is the critical ferric: ferrous ion ratio at which the rate transitions from high to low rates.

A dynamic analysis for the bioleaching of chalcopyrite in a batch reactor was performed by substituting the ferric and ferrous ion material balances into Eq. 5. Pseudo-steady state(s) with respect to the redox potential R were identified when Eq. 5 was equated to zero (Eq. 8) to reveal up to three pseudo-steady states when a microbial oxidation rate developed by Hansford[14] (Eq. 6), and an empirical leaching rate expression developed by Petersen and Dixon[15] (Eq. 7), and was used in the analysis

$$\underbrace{(R+1) \cdot r_{Fe^{2+}}}_{r_M} = \underbrace{(\beta R + \alpha) \cdot r_{MS}}_{r_L^B} \quad (8)$$

where α and β are the stoichiometric coefficients of the ferric and ferrous ions in solution according the chemical leaching reaction (Eq. 1), respectively, $r_{Fe^{2+}}$ [mol m^{-3} s^{-1}] r_{MS} and [mol m^{-3} s^{-1}] the microbial oxidation and chemical leaching intrinsic rates, and for simplicity, the microbial oxidation $(R+1)r_{Fe^{2+}}$ and chemical leaching $(\beta R + \alpha)r_{MS}$ rate functions for the batch system are assigned as r_M and r_L^{β}, respectively.

To simplify the dynamic analysis, it was assumed that during the batch bioleach process, the particle surface area was constant. However, it was noted that the actual particle surface area could be predicted by means of the modified PBM approach outlined in earlier work.[2]

In this study, we attempt to derive a method for analyzing bioleaching dynamics in continuous flow systems using the constant particle surface area assumption. Thereafter, the dynamic analysis in continuous flow systems will be extended to include the particle shrinkage effects by incorporating the PBM using a segregation approach introduced earlier.

Continuous Flow Bioleach Dynamics

When modeling continuous flow reactors, it is assumed that particles fed to the reactor are instantly perfectly mixed with the other particles already present. The fluid phase concentrations and temperature in the vicinity of each particle in the reactor are therefore considered to be the same. The reactor is normally operated at steady hydrodynamic conditions and since it is assumed to be perfectly mixed, the conditions in the exit stream from the reactor are identical to those inside the reactor.

Due to the system being in a state of continuous flow, the transient change in ferric and ferrous ions is dependent on the mean residence time in the reactor. In performing a dynamic analysis, we first develop the unsteady-state balances describing system evolution (Eqs. 9 and 10)

$$\frac{dC_{Fe^{3+}}}{dt} = \frac{C_{Fe^{3+}_{\text{inlet}}} - C_{Fe^{3+}}}{\tau} - \alpha r_{MS} + r_{Fe^{2+}} \tag{9}$$

$$\frac{dC_{Fe^{2+}}}{dt} = \frac{C_{Fe^{2+}_{\text{inlet}}} - C_{Fe^{2+}}}{\tau} - \beta r_{MS} + r_{Fe^{2+}} \tag{10}$$

where τ [s] is the mean particle residence time and, $C_{Fe^{3+}_{\text{inlet}}}, C_{Fe^{2+}_{\text{inlet}}}$ and $C_{Fe^{3+}}, C_{Fe^{2+}}$ [mol m^{-3}] are the inlet and outlet concentrations of the ferric and ferrous ions, respectively. Since our focus in this section is on the chemistry and not the hydrodynamics of the system, the inlet and outlet flow rates to and from the reactor are assumed constant, and, hence, the mean residence time τ [s] is also constant. Scenarios in which the flow rates are not constant, and, hence, the mean residence time is a function of time, will be investigated in a future study.

Substituting the material balances in Eqs. 9 and 10 into Eq. 5 and simplifying, yields the transient change in solution redox potential R for a continuous flow bioleach reactor (Eq. 11)

$$\frac{dR}{dt} = \frac{(R+1)\cdot r_{Fe^{2+}} - (\beta R + \alpha)\cdot r_{MS}}{C_{Fe^{2+}}} - \frac{C_{Fe^{3+}_{\text{inlet}}}\left(1 - \frac{R}{R_{\text{inlet}}}\right)}{\tau C_{Fe^{2+}}} \tag{11}$$

where R_{inlet} is the inlet ferric/ferrous ion ratio to the continuous stirred-tank bioleach reactor.

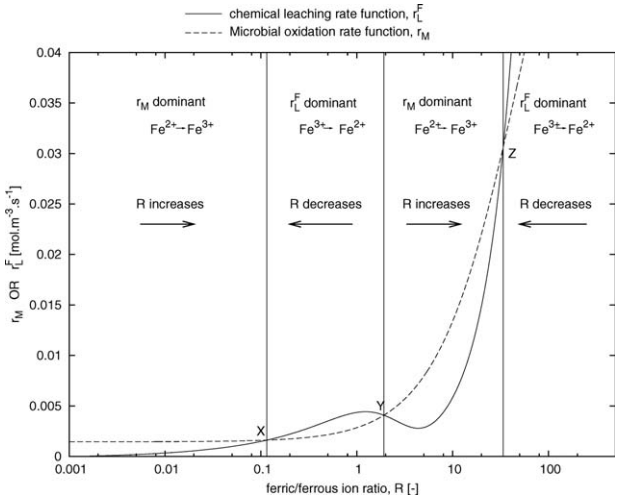

Figure 1. Dynamic analysis of chalcopyrite bioleaching in continuous flow systems.

Steady states exist at the intersection of the rate function curves. The solid curve indicates the chemical leaching rate function, and the dotted curve the microbial oxidation rate function r_M in Eq. 12.

Steady state(s) with respect to R for the continuous flow bioleach reactor are obtained when the LHS in Eq. 11 is zero (Eq. 12). From Eq. 12 we note that the first term on the RHS is the familiar batch term derived in Eq. 8, while the second term is the change in the ferric:ferrous ion ratio R resulting from flow into and out of the bioleach reactor of the principal ferric and ferrous ions

$$\underbrace{(R+1)\cdot r_{Fe^{2+}}}_{r_M} = \underbrace{(\beta R + \alpha)\cdot r_{MS} - \frac{C_{Fe^{3+}\text{inlet}}}{\tau}\left(1 - \frac{R}{R_{\text{inlet}}}\right)}_{r_L^F} \tag{12}$$

where the microbial oxidation rate function on the LHS and the chemical leaching rate function on the RHS of Eq. 12 for the bioleach flow system will, from this point onward, be referred to by r_M and r_L^F, respectively.

The dynamic analysis of the flow reactor is analogous to the batch case; steady state(s) are the points of intersection between the microbial oxidation rate function curve $(R+1)r_{Fe^{2+}}$ and the chemical leaching rate function curve $(\beta R + \alpha)r_{cpy}$, excepting that the latter term must be offset by the flow contribution $-\frac{C_{Fe^{3+}\text{inlet}}}{\tau}\left(1 - \frac{R}{R_{\text{inlet}}}\right)$ (Figure 1).

In any region in Figure 1 where the microbial oxidation rate function r_M lies above the chemical leaching rate function r_L^F, ferrous ions are converted to ferric ions (Eq. 12). In this region, the overall rate shifts to higher redox potentials (R increases, see Figure 1) where a steady state is observed at the intersection of the rate curves at points X and Z in Figure 1. However, when chemical leaching (Eq. 1) is the dominant reaction, the overall rate shifts to lower ferric:ferrous ion ratios (R decreases, see Figure 1). In the case of chalcopyrite bioleaching, stable steady states are observed at low X and high Z redox potentials. The intersection Y observed between these rate curves is an unstable steady state, since dominating microbial oxidation and chemical leaching reactions are observed at redox potentials to the left and right of this intersection point, respectively, which shift

the overall rate to lower X or higher Z ferric:ferrous ion ratios, respectively. In other words, in the vicinity of Y, unless the initial state is exactly on Y, the system tends to fall away from R_Y. As with the batch system,[1] the dynamic analysis of chalcopyrite bioleaching in the continuous flow system reveals two stable steady states at low X and high Z ferric:ferrous ion ratios with an unstable steady-state Y at intermediate redox potentials.

Up to this point, the dynamic analysis was developed under a fixed particle surface area assumption, regardless of the disappearance of mineral from the particle due to reaction. For more accurate analysis, however, this assumption has to be relaxed and a population balance has to be integrated into the formulation.

Continuous Flow Bioleach Dynamics: Application of the Modified PBM

In the previous sections, the reactor volume-based leaching rate r_{MS} in Eqs. 11 and 12 was assumed to be equivalent to the intrinsic leaching rate of chalcopyrite in Eq. 7 multiplied by the fixed reactor-volume based particle specific surface area A^v [$m^2\ m^{-3}$] which is the product of the particle specific surface area A^P [$m^2\ kg^{-1}$] with particle mass M^P [kg] relative to the reactor volume V^R [m^3] (Eq. 13)

$$A^V = \int_0^\infty \int_0^\infty A^p(\theta, l_0) \frac{M^p(\theta, l_0)}{V^R} N^T I(\theta) f_0(l_0) d\theta dl_0 \qquad (13)$$

These studies were used to establish a basis for the dynamic analysis without the complicating influence of time-varying particle surface area changes. Now that the procedure is established, the more rigorous analysis must be performed.

The leaching rate r^R [$mol\ m^{-3}\ s^{-1}$] in Eq. 3 is a function of the particle specific surface area A^P [$m^2\ kg^{-1}$], particle residence time or age θ [s], inlet particle size l_0 [m], and the intrinsic leaching rate $r'' = r_{MS}$ [$mol\ m^{-2}\ s^{-1}$] [2]. Accepting that there exists a distribution in age I (θ) [s^{-1}] within the reactor, and that a nontrivial distribution of particle size f_0 (l_0) [m^{-1}] applies to the reactor feed, the overall leaching rate, and, hence, the dynamic analysis for the flow system with changing particle size can be determined (Eq. 14)

$$r^R = \phi_{MS} \cdot r_{MS} A^V \qquad (14)$$

Since the intrinsic leaching rate is reported on a surface area basis, the particle leaching rate will be the product of the intrinsic leaching rate with the particle specific surface area, which itself is a function of the particle residence time and inlet size.[2] The dynamic analysis for bioleaching mineral sulfide ores, therefore, indicates a shift in steady state due to the time-varying particle surface area, and is expected to yield different results from the analysis for a continuous flow system with the fixed surface area assumption.

The time-varying change in particle surface area due to leaching is incorporated in the overall leaching rate r^R (Eq. 12). The intrinsic leaching rate r_{MS} in Eq. 3, multiplied by the particle specific surface area (Eq. 12), in the dynamic analysis for a continuous bioleach system is consequently equivalent to the overall leaching rate r^R in Eq 3 (Eq 15)

$$\underbrace{(R+1) \cdot r_{Fe^{2+}}}_{r_M} = \underbrace{(\beta R + \alpha) \cdot r^R - \frac{C_{Fe^{3+}\text{inlet}}}{\tau}\left(1 - \frac{R}{R_{\text{inlet}}}\right)}_{r_L^S} \qquad (15)$$

where r_L^S is the overall chemical leaching rate function that incorporates a time-varying particle surface area due to reaction and flow.

Now that a model has been developed, a rigorous dynamic analysis for the bioleaching of chalcopyrite bioleaching can be performed in continuous flow systems. Process variables which influence the dynamics of the system will be identified using a sensitivity analysis applying the constant surface area assumption. This assumption will then be relaxed to incorporate a reaction rate that includes the change in particle surface area.

Sensitivity Analysis

In order to exploit the dynamics to achieve high-bioleaching rates, the sensitivity of the rates involved to all factors should be examined. It is evident from Eqs. 12 and 15 that these operating parameters may include the biomass concentration C_X, which directly affects the microbial oxidation rate (Eq. 1), the mean residence time τ and the inlet ferric:ferrous ion ratio R_{inlet}. An increase or decrease in any of these parameters will shift either or both of the rate curves resulting in a change to the dynamic structure of the system.

In the following sections, a dynamic analysis for the bioleaching of chalcopyrite will be undertaken to determine the influence of the aforementioned process variables on the dynamic structure of the system. Initially, the dynamic analysis will use the constant particle surface area assumption to compare the influence of mean residence time on steady operation in a CSTR. Thereafter, this assumption will be relaxed by incorporating the modified PBM approach in the dynamic analysis that considers particle surface area changes with reaction. Kinetic constants applied in the sensitivity analysis using the constant surface area assumption are reported in Table 1. The chemical leaching rate constants A and B are obtained from the Arrhenius terms developed by Kotsiopoulos et al.[1] at 343.15 K from the chemical leaching experiments performed by Kametani and Aoki[17] while microbial oxidation rate constants $q^{\max}_{Fe^{2+}}$ and K were assumed to follow a Arrhenius relationship established by Searby.[22]

Influence of Biomass

The microbial oxidation rate is directly proportional to the biomass concentration C_X (Eq. 6). As such, increases in C_X can be represented graphically by an upward shift in the rate curve from L_1 to L_3 in Figure 2 with corresponding biomass concentrations C_X,1 to $C_{X,3}$, respectively. The microbial oxidation rate function curve passes from a single intersection between L_1 and the chemical leaching rate function curve at low-solution redox potentials to multiple intersections between L_2 (at biomass concentration $C_{X,2}$) and the leaching rate curve. Finally, a single intersection L_3 is observed at high ferric:ferrous ion ratios with increasing biomass concentration, thus, changing the dynamics structure of the system. This change in dynamic structure due to any change in a process variable is known as a bifurcation.

Biomass concentrations below $C_{X,a}$ and above $C_{X,b}$ (corresponding to curves L_a and L_b in Figure 2, respectively) are critical values at which the dynamics picture for the system changes from a 3-steady state case to a single stable steady state. Points $C_{X,a}$ and $C_{X,b}$ are, therefore, bifurcation points. Graphically, bifurcation points $C_{X,a}$ and $C_{X,b}$ with corresponding ferric:ferrous ion ratios $R_{a,B}$ and $R_{b,B}$, respectively occur when the microbial oxidation and chemical leaching

Table 1. Chemical Leaching and Microbial Oxidation Rate Constants Utilized in the Dynamic Analysis for a Continuous Flow System Applying the (a) Constant Particle Surface Assumption, and (b) a Time-Varying Particle Surface Area by Incorporating the Modified PBM[2]

Chemical Leaching Rate Constants			Microbial Oxidation Constants	
A	B	R_{crit}	$q^{max}_{Fe^{2+}}$	K
(a) Constant Particle Surface Area				
1.27×10^{-3} [mol m^{-3} s^{-1}]	2.5×10^{-5} [mol m^{-3} s^{-1}]	1	3.02×10^{-3} [mol Fe^{2+} mol^{-1} carbon s^{-1}]	0.019
(b) Time-Varying Particle Surface Area				
1.63×10^{-7} [mol m^{-2} s^{-1}]	3.2×10^{-9} [mol m^{-2} s^{-1}]	1	3.02×10^{-3} [mol Fe^{2+} mol^{-1} carbon s^{-1}]	0.019

rate function curves are tangent and equal to each other. Mathematically bifurcation points can be obtained when the rate functions r_M and r_L^F, as well as, the gradients with respect to R, are equal (Eqs. 12 and 16)

$$\frac{d\left[(\beta R+\alpha)\cdot r_{MS}-\frac{C_{Fe^{3+}\text{inlet}}}{\tau}\left(1-\frac{R}{R_{\text{inlet}}}\right)\right]}{dR}=\frac{d[(R+1)\cdot r_{Fe^{2+}}]}{dR} \tag{16}$$

The phase plane presented in Figure 2b is generated by varying the biomass concentration C_X and re-evaluating the steady states at the corresponding ferric:ferrous ion ratios R. A characteristic S-shaped curve with bifurcation points $C_{X,a}$ and $C_{X,b}$ is obtained. The dynamic analysis on the continuous bioleach reactor reveals similar trends to those observed in the batch system.[1] If a phase plane of steady states for the bioleaching of chalcopyrite are plotted for the continuous flow bioleach reactor together with pseudo-steady states observed for a batch system for given steady-state microbial concentrations, the influence of flow can readily be understood (Figure 3).

The phase plane for the continuous flow bioleach reactor was generated for a reactor operating with a mean residence time of $\tau = 2$ days. In Figure 3, it can be seen that when bioleaching chalcopyrite in either a batch or continuous flow reactor, steady states are achieved at slightly different overall solution redox potentials for the same biomass concentrations (viz. R_a^B, R_b^B and $C_{X,a}^B$, $C_{X,b}^B$ for the batch reactor and R_a^F, R_b^F and $C_{X,a}^F$, $C_{X,b}^F$ for the continuous flow reactor in Figure 3). The similarities in the two dynamics trends in Figure 3b is due to the first term on the RHS of Eq. 11, the batch term, being much greater than the second term on RHS of Eq. 11, the flow term for a mean residence time of 2 days. The magnitude of the flow term is directly proportional to the ferric ion concentration in the feed stream to the CSTR and inversely proportional to the mean residence time. The greater the inlet ferric ion concentration to the continuous flow system, and the smaller the mean residence time, the more pronounced the differences between pseudo-steady states in the batch and steady states in a continuous flow bioleach reactors are. Using low-flow rates (hence, large residence times) would result in a system which operates close to batch operation and, hence, it would be expected that when the flow rate is reduced, the CSTR curve approximates the batch curve.

Influence of mean residence time

In order to determine the influence of the mean residence time on the dynamic analysis of the continuous flow bioleach reactor, mean residence times 0.5, 0.75, 1, 2, 5 and 10 days were simulated and the steady-state curves plotted together with that for a batch reactor (Figure 3b). Figure 3b reveals that

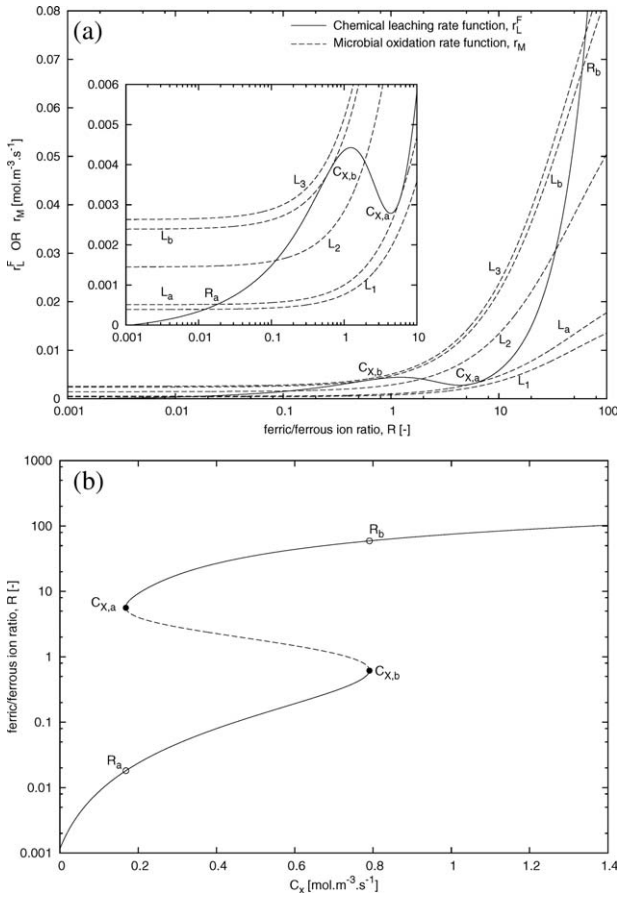

Figure 2. Chemical leaching rate function with a family of microbial oxidation rate function curves r_M with biomass concentrations $C_{X,1}$, $C_{X,2}$ and $C_{X,3}$ corresponding to curves L_1, L_2 and L_3, respectively, and concentrations $C_{X,a}$ and $C_{X,b}$, correspond to curves L_a and L_b, respectively.

$C_{X,a}$ and $C_{X,b}$, are the bifurcation points. The microbial oxidation rate function curve r_M shifts upward with increasing biomass concentration $C_{X,1} < C_{X,2} < C_{X,3}$. Single steady states occur when the biomasss concentration is less than $C_{X,1}$, L_1 and greater than $C_{X,3}$, L_3. Multiple points of stability are observed when the concentration is $C_{X,2}$, L_2. Low-bioleaching rates occur when one intersection point is observed L_1, L_3. Solid curves in the R-X plane in Figure 2b indicate stable steady states, and the dotted curve unstable steady states.

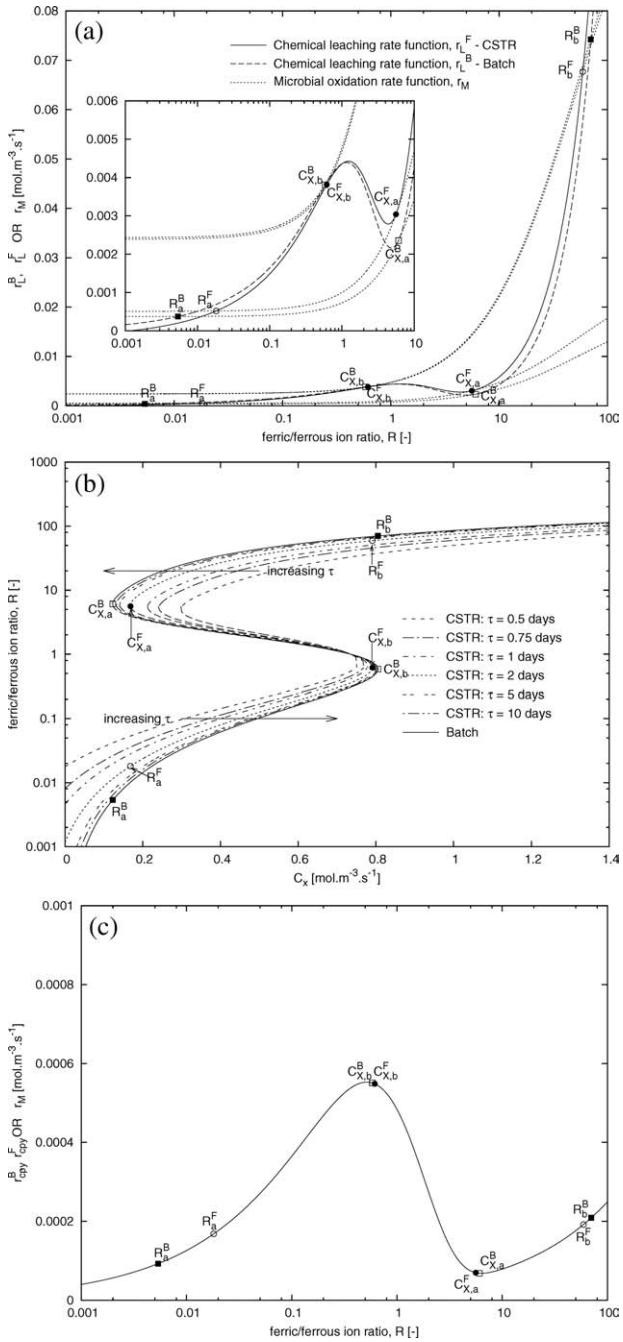

Figure 3. (a) Comparison of the dynamic analysis of chalcopyrite bioleaching in a batch reactor and a CSTR.

The influence of the mean residence time τ on the points of stability and the ferric:ferrous ion ratio R in a continuous flow system are presented in (b), parameters superscripted with F and B refer to flow (CSTR) and batch reactor systems, respectively. Reaction rates are determined from the chemical leaching rate curve at the corresponding redox potentials R shown in (c).

as the mean residence time in the continuous flow reactor is increased the system approaches batch operation. This is expected since large mean residence times would eliminate the flow term in Eq. 11, thus, driving the system to batch operation (Eq. 8).

Steady states in the CSTR at redox potentials below the bifurcation biomass concentration $C^F_{X,b}$ equilibrate at higher ferric:ferrous ion ratios than those achieved in the batch reactor (viz. R^B_a and R^F_a for the batch reactor and CSTR, respectively, in Figure 3), while steady operation occurs at lower redox potentials for ferric:ferrous ion ratios above bifurcation biomass concentration $C^F_{X,a}$ than in the batch reactor (viz. R^B_b and R^F_b for the batch and continuous flow reactors, respectively, in Figure 3). This implies that high-overall bioleaching rates can be achieved at higher solution redox potentials in the CSTR than in the batch reactor, while the critical ferric:ferrous ion ratio prior to the system transitioning to low-bioleaching rates (Figure 3c) remains relatively constant at bifurcation biomass concentrations $C^F_{X,b}$, $C^B_{X,b}$. However, low rates are observed at lower ferric: ferrous ion ratios that are above bifurcation biomass concentration $C^F_{X,a}$ than at equivalent points in the batch system, hence, requiring a higher microbial activity (viz. points R^B_a and R^F_a for the batch reactor and CSTR, respectively, in Figure 3c).

Influence of ferric:ferrous ion ratio

Up to this point the system dynamics has focussed on the influence of the steady state ferric:ferrous ion ratio R on the dynamic structure of the system (Eqs. 8, 12 and 15). This analysis is not sufficient to determine the system steady state since the redox potential continuously increases with microbial oxidation, thus, driving the bioleaching reaction to high ferric:ferrous ion ratios, where low-overall steady-state bioleaching rates are observed. The biomass concentration C_X explicitly appears in the ferric:ferrous ion ratio R balance in Eq. 15 via the microbial oxidation rate expression $r_{Fe^{2+}}$ (Eq. 15), which implies that steady state is only possible when both C_X and R are at steady state. As such, the dynamics associated with biomass growth also needs to be developed. To determine the dependence of the system on the biomass concentration we first develop the unsteady-state mass balance over the continuous flow bioleach reactor (Eq. 17)

$$\frac{dC_X}{dt} = \frac{C_{X,\text{inlet}} - C_X}{\tau} + Y_{XS} r_{Fe^{2+}} \tag{17}$$

where $C_{X_{\text{inlet}}}$ and C_X [mol carbon m^{-3}] are the inlet and outlet biomass concentrations, respectively, and Y_{XS} is the biomass yield defined as the moles of biomass produced per mole of substrate.

The biomass concentration in a flow system increases proportionally with the rate of ferrous ion consumption. Since no biomass is present in the inlet stream to the reactor ($C_{X,\text{inlet}} = 0$) and incorporating the microbial oxidation reaction rate expression (Eq. 6), the steady-state conditions applied to Eq. 17 yields Eq. 18

$$R_S = \frac{Y_{XS} q^{\max}_{Fe^{2+}} \tau - 1}{K} \tag{18}$$

where the subscript "s" is introduced to emphasize that these are the steady-state values. This equation gives an additional constraint which when coupled with the locus of possible steady states on the R-X plane (Figure 4a), yields the single possible steady-state R value R_S.

Figure 4 was generated to demonstrate the influence of the inlet ferric:ferrous ion ratio to the reactor (Figure 4a and b, and the initial ferric:ferrous ion ratio inside the

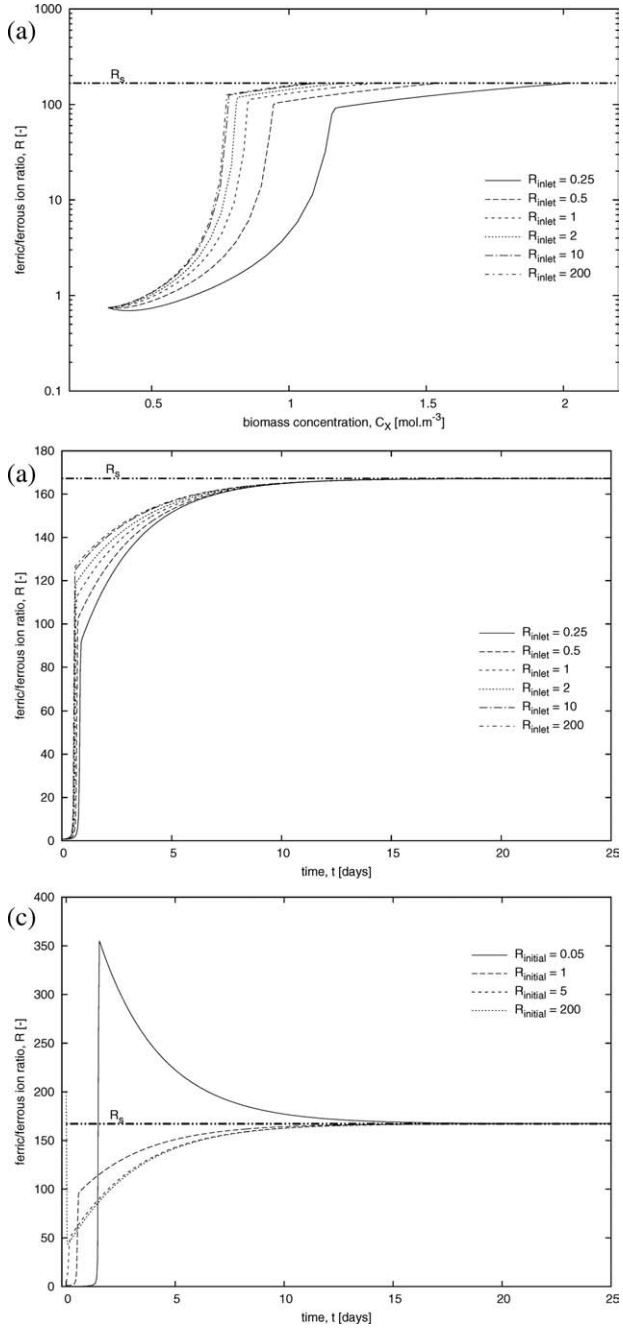

Figure 4. Steady-state ferric:ferrous ion ratios *R*. Only a single stable steady state is achieved at R_s = 167.2 for a mean residence time τ = 2 days when either the inlet R_{inlet} (a) and (b), or initial $R_{initial}$ (c) ferric:ferrous ion ratio is varied.

bioleach reactor (Figure 4c) on stable steady states in a flow reactor system with changing particle surface area. Ratios ranging from 0.25 to 200 were investigated. The time profile for the ferric:ferrous ion ratio R was determined by integrating Eq. 11 assuming a 2 day mean residence time. Regardless of the inlet conditions to the reactor or the initial ferric:ferrous ion ratio inside the reactor, the system always shifted to a single steady-state R value in the high ferric:ferrous ion ratio region, confirming that the system operating point is determined by the ferric:ferrous ion ratio R_s (Eq. 18).

Influence of time-varying particle surface area

The preceding sensitivity analyses determined the influence of varying the biomass concentration, mean residence time and inlet ferric:ferrous ion ratio on the dynamic structure of the system without the application of a time-varying particle surface area. In reality, the degree to which particle mass is liberated into the aqueous phase is influenced by the rate of reaction and particle-solution contact time. This change in mass relates to a change in particle surface area and should be incorporated into the dynamic analysis to determine its influence on system steady states. This influence is presented in Figure 5 by means of comparing the steady states achieved in a batch reactor (Eq. 8), and a continuous flow reactor with (Eq. 15) and without (Eq. 12) the application of time-varying particle surface area by incorporation of the developed PBM.

The dynamic analyses in the following, and subsequent sections, were performed assuming a mean particle size of 12.5×10^{-6} m, and 2 days mean residence time under conditions of perfect mixing in the reactor. Kinetic constants A and B for the intrinsic leaching rate in Eq. 7 and the maximum microbial specific ferrous iron utilization rate $q^{max}_{Fe^{2+}}$, and inhibition constant K for the microbial oxidation rate in Eq. 6 applied in the dynamic analysis are reported in Table 1.

In Figure 5 it can be seen that steady states for the continuous flow system, as predicted using the overall leaching rate r^R formulated in Eq. 3, are obtained at lower biomass concentrations than in analyses that do not consider particle surface area changes. As explained before, the overall leaching rate will decrease as the reaction proceeds. This decrease in the leaching rate is graphically presented in Figure 6 (viz. $C^S_{X,b}$ and $C^F_{X,b}$ for the continuous flow reactor with and without the application of time-varying particle surface area, respectively) by a downward shift in the rate function to lower overall rates at the corresponding redox potential.

Now that the influence of biomass concentration, solution redox potential, mean residence time and time-varying particle surface areas on the dynamic analysis is known and the

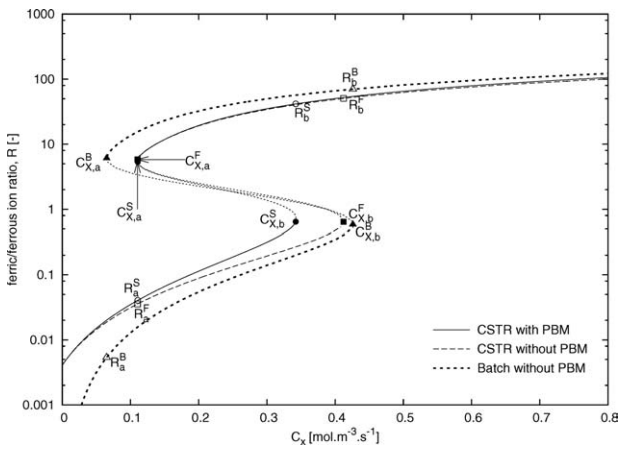

Figure 5. Comparison of steady states achieved during the bioleaching of chalcopyrite in a batch and CSTR.

The valuesandindicate bifurcation points. Parameters superscripted with *F* and *B* refer to flow (CSTR) and batch reactor systems, respectively, with the constant particle surface area, while parameters with superscript *S* refer to a flow reactor (CSTR) with time-varying particle surface area by application of the modified PBM.

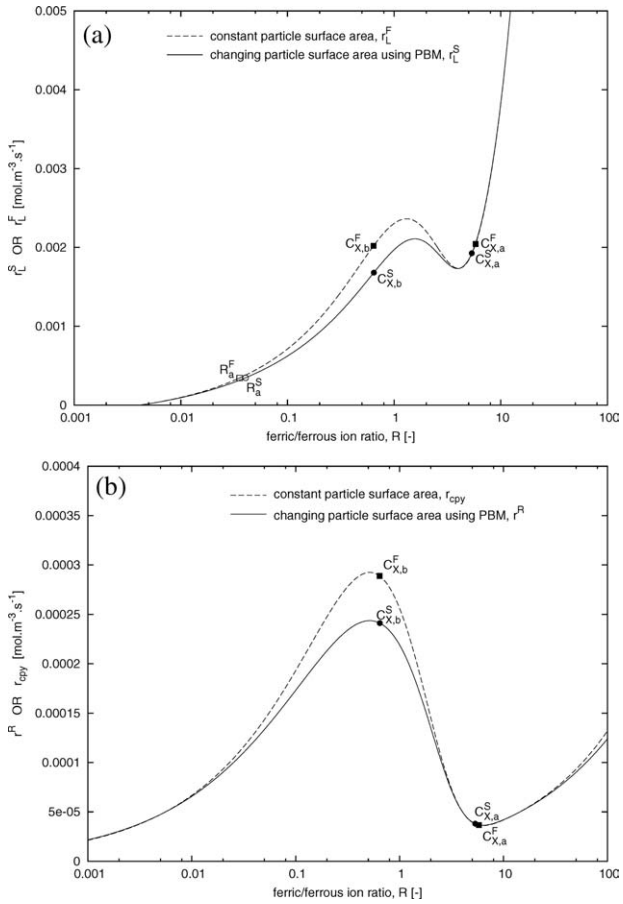

Figure 6. (a) Comparison of the leaching rate for a CSTR with and without the application of particle surface area changes, and actual leaching rates are shown in (b).

critical regions have been identified in the light of a dynamic analysis, practical outcomes such as obtaining high-bioleaching rates can be investigated.

Optimization

To optimize plant operation the process variables required to maximize production yield need to be identified. Optimum plant operation is typically achieved by maximizing the overall reaction rate. In bioleaching, valuable metals are obtained by means of the acid-ferric leaching of the mineral sulfide ore (Eq. 1). To achieve maximum product output the overall chemical leaching rate (Eq. 3) must be at a maximum, thus, making the overall chemical leaching rate an important optimization parameter.

From the dynamic analysis we are able to identify operating conditions which maximize the overall reaction rate. In Figures 2 and 6, maximum rates are obtained at intermediate ferric:ferrous ion ratios about $R = 1$, while low rates are achieved at ferric:ferrous ion ratios $R > 1$. From these figures, it is clear that to maintain the rate at the maximum value, the microbial oxidation and chemical leaching rate curves must be tangent and equal to each other which, in this case, coincides with the bifurcation point $C_{X,b}$.

As previously noted, bifurcation points indicate a single branch of stable steady states prior to ($C_{X,a}$ in Figure 2), and after which ($C_{X,b}$ in Figure 2) the bioleaching system transitions from a three steady-state regime to, again, a single branch of stable steady-state operation. As such, with regard to system stability, the maximal rate point is actually in an undesirable location since operating near a bifurcation may cause the system to fall away from the design operating point when even small fluctuations occur in the inputs or operating conditions.

Referring to rate curve L_b in Figure 2, we noted high rates at point $C_{X,b}$ with low rates at ferric:ferrous ion ratio R_b. Since the microbial oxidation rate curve L_b in Figure 2 is directly proportional to the biomass concentration (Eq. 6), any biomass concentration greater than $C_{X,b}$ would result in a single intersection of the microbial oxidation and chemical leaching rate curves at high ferric:ferrous ion ratios R shifting the system to low-stable steady-state rates (see rate curve L_3 in Figure 2). It is clear that when bioleaching chalcopyrite, maximum stable steady-state rates can be obtained at point $C_{X,b} = C_{X,\max}$ (Figures 3 and 6) which is sensitive to any small changes in the biomass concentration. Any increase in the biomass concentration $C_X > C_{X,b}$ would shift the system to low rates, therefore, when developing a control strategy to maintain high-bioleaching rates, the biomass concentration should never exceed $C_{X,b}$.

Optimum operating conditions C_X and R, where maximum bioleaching rates are achieved, which explicitly appear in the microbial oxidation rate expression $r_{Fe^{2+}}$ (Eq. 6), can be determined using Eqs. 15 and 16 and are illustrated in Figure 7 as a function of mean residence time. Figure 7

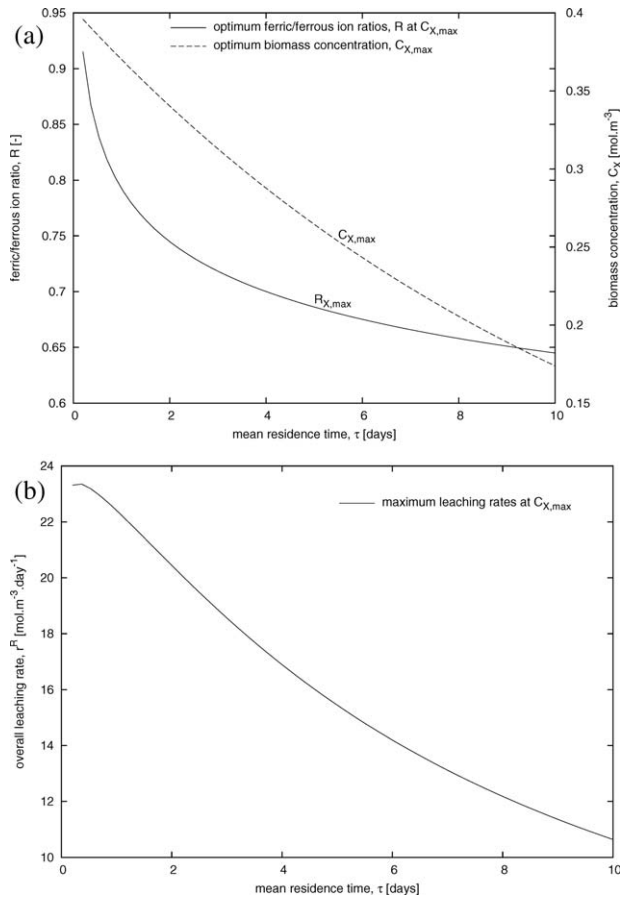

Figure 7. Locus of optimum (a) biomass concentrations $C_{X,a}$ with corresponding ferric:ferrous ion ratios $R_{X,a}$, and (b) maximum bioleaching rates r^R as a function of mean residence time τ.

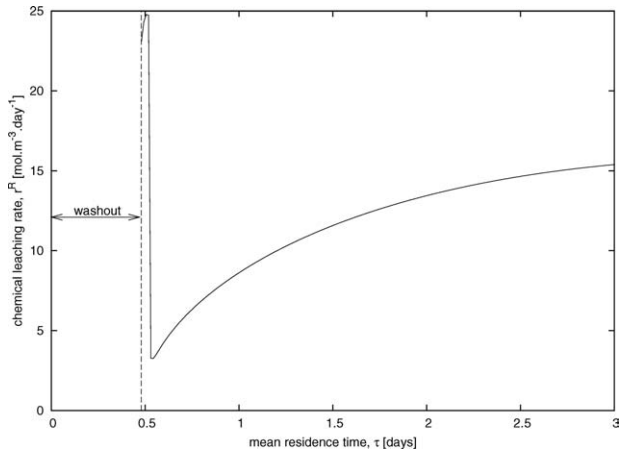

Figure 8. The overall chemical leaching rate r^R achieved when the reactor mean residence time is reduced from 2 days to 0.48 days.

Washout occurs when $\tau \leq \frac{1}{Y_{XS}q^{\max}_{Fe^{2+}}}$.

reveals that the optimum biomass concentrations $C_{X,\max}$ and ferric:ferrous ion ratios $R_{X,\max}$ (Figure 7a), where maximum rates are realized (Figure 7b), decrease with increasing mean residence time.

As previously stated, optimum operating conditions to sustain maximum rates for the bioleaching of chalcopyrite unfortunately coincide with the system bifurcation point. Thus, maintaining maximum rates at these conditions would require precise control systems that keep the biomass concentration at $C_{X,\max}$. If $C_{X,\max}$ is exceeded, the system would transition from high to low rates. It is, therefore, necessary that the biomass concentration is controlled to within some margin below $C_{X,\max}$ to ensure that high rates are maintained.

Control

In the following section, control strategies to achieve maximum rates are introduced. Figure 7 revealed that the highest rates are obtained at high-flow rates or low-mean residence times, while the sensitivity analysis revealed that a critical concentration exists prior to the system shifting from high-overall rates at intermediate ferric:ferrous ion ratios to low rates at high ferric:ferrous ion ratios (Figure 2). The challenge is, therefore, to keep the system at an optimum by controlling the relevant process variables. From the dynamic analysis for a continuous flow system, it is clear that maximum rates can be achieved by either controlling the reactor mean residence time or the biomass concentration.

In the following section, control procedures to keep the system at high-bioleaching rates are proposed.

Mean residence time

From the sensitivity analysis, it was determined that the system operating point is determined by the reactor concentration ferric:ferrous ion ratio R_s and not by the inlet or initial ferric:ferric ion ratio. Since a single R value exists in both space and time, there is only one stable steady state, therefore, maintaining maximum rates at $C_{X,\max}$ in a single bioleach reactor can, according to Eq. 18, only be achieved by adjusting the reactor mean residence time τ [s]. For example, if $C_{X,\max} = 0.34$ mol carbon m^{-3} with $R_{X,\max} = 0.65$ for a given reactor mean residence time $\tau = 2$ days in Figures 3b and 5, the required mean residence time would be $\tau = 0.48$ days to achieve the desired rate (Figure 8), which deviates from the 2 days mean residence time. In Figure 8, the overall chemical leaching rate is at a maximum at $\tau = 0.48$ days. Thereafter, the rate increases with increasing mean residence time. It should be noted that at mean residence times $\tau \leq \frac{1}{Y_{XS}q^{\max}_{Fe^{2+}}}$, R_S is less than zero (Eq. 18). At these mean residence times, the growth rate is less than the dilution rate and washout of the biomass occurs (Figure 8).

Operating at this mean residence time would ensure high-bioleaching rates. However, the conversion per tank would be low due to the diminished reaction space-time (Figure 8). As a result, the same overall conversion obtained for a reactor with mean residence time $\tau = 2$ days could be achieved using quarter sized tanks in series operating at maximum extraction rates.

From Eq. 18 we note that the system will always shift to ferric:ferrous ion ratios R that do not give the optimal leaching rate. Maximum leaching rates could be obtained when the reactor mean residence time was reduced. The reason for the rate enhancement is that any excess biomass that shifts the system to low rates at high-redox potentials is washed out. However, since the biomass is generally thought to be uniformly suspended in the solution, lower residence times also result in reduced macroproductivity.

Although reducing the mean residence time results in higher productivity, the system will be operated near the washout point (Figure 8). Any fluctuations in the system flow rates may result in complete washout and, therefore, eliminate any microbial activity driving the system to low-overall rates.

It is only through the dynamic analysis that the appropriate mean residence times to achieve high rates could be identified. The analysis revealed that increasing the system flow rate or reducing the reactor mean residence time, would control microbial growth and, hence, maintain the system at maximum rates.

Biological stress

The chemical leaching rate of chalcopyrite increases with increasing ferric/ferrous ion ratio until it reaches a maximum at a critical ferric:ferrous ion ratio, after which the rate decreases (see Figure 1). From the sensitivity analysis we noted that a critical biomass exists prior to the system switching from increasing to decreasing rates near the critical ferric:ferrous ion ratio (Figure 2). It is clear that to operate the bioleach reactor at high rates, the biomass concentration should be kept at levels below the critical biomass concentration. This was further emphasized in the previous section where the mean residence time was used to control the biomass concentration. Although the biomass in the system promotes leaching, it emerged that restricting the biomass concentration levels to below the critical value resulted in higher overall rates. This outcome opens new possibilities in enhancing the achieved reaction rate. Reducing the biomass concentration in the reactor by introducing biological stress factors, such as high-shear stress rates or solids loading[18–21] would suppress the biomass concentration to below the critical point $C_{X,b}$ (Figures 3 and 6) and keep the system at ferric:ferrous ion ratios R within the optimal operating range. In stirred-tank reactors biological stresses are induced by high-agitation rates and the inclusion of abrasive particles.[20] An increase in either of these physical phenomena

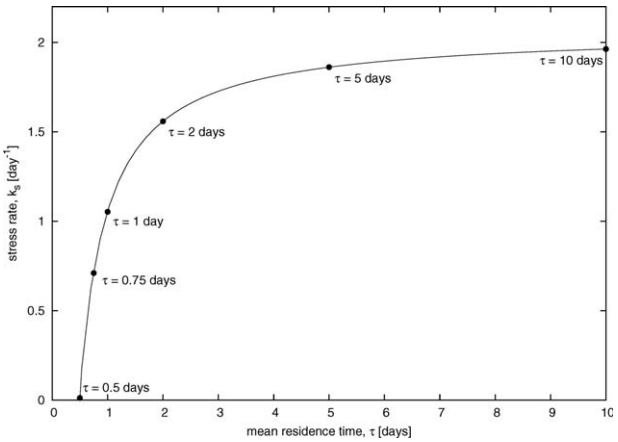

Figure 9. Hydrodynamic stress rate k_s required to maintain maximum overall bioleaching rates r^R as a function of reactor mean residence time τ.

promotes cell stress and could be used to control the biomass concentration in a reactor. If applied to the system assuming a first-order stress rate, the biomass balance in Eq. 17 is rewritten as Eq. 19

$$\frac{dC_X}{dt} = \frac{C_{X,\text{inlet}} - C_X}{\tau} + Y_{XS} r_{Fe^{2+}} - k_s C_X \tag{19}$$

where k_s [s^{-1}] is the microbial stress rate. The value of k_s can be correlated to the applied stress rate due to agitation and abrasive solids loading.

If the desired biomass concentration $C_{X,\max}$ and ferric:ferrous ion ratio $R_{X,\max}$ is known, the required steady-state stress rate k_s to obtain maximum leaching rates can be calculated (Eq. 20). At steady state, the relationship in Eq. 20 is observed

$$k_s = \frac{Y_{XS} q^{\max}_{Fe^{2+}}}{(1+KR)} - \frac{1}{\tau} \tag{20}$$

The stress rates k_s needed to obtain maximum rates at biomass concentrations $C_{\text{X,max}}$ and corresponding ferric/ferrous ion ratio $R_{X,\max}$ is shown in Figure 9. As expected the required stress rate to sustain the system at maximum bioleaching rates is higher at high-mean residence times since more biomass accumulates in the reactor as the system approaches batch operation (Figures 3b and 9, Eq. 15).

When applying the optimal stress rate, an effective control procedure can be identified with the objective of maintaining high-bioleaching rates. If the reactor operates at a mean residence time $\tau = 2$ days, with maximum rates at $C_{X,\max} = 0.34$ mol carbon m^{-3} and $R_{X,\max} = 0.65$ (Figure 5) the required stress rate to maintain the optimum operating point can be calculated from Eq. 20. The leaching rate decreases as the applied stress rate increases until the optimum ferric:ferrous ion ratio is achieved at $R_{X,\max} = 0.65$. At this point the biomass concentration required to maintain maximum rates is at an optimum (see Figure 5). This is indicated in Figure 10 by the sharp increase in the leaching rate at $k_s = 1.81 \times 10^{-5}$ s^{-1}. With a stress rate $k_s = 1.81 \times 10^{-5}$ s^{-1}, it can be seen in Figure 10 that the overall bioleaching rate increases by 56% compared to a system that does not incorporate any biological stress ($k_s = 0$ s^{-1}).

From the dynamic analysis of chalcopyrite bioleaching in a flow system, we note that in addition to the biomass concentration C_X and ferric:ferrous ion ratio R, the inlet ferric ion concentration $C_{Fe^{3+}_{\text{inlet}}}$ and reactor mean residence time τ directly affects the dynamic structure of the system. The latter parameters affect the magnitude by which the chemical leaching rate function r^S_L is offset by the flow term in Eq. 15, thereby shifting the system to lower rates.

By performing a dynamic analysis, factors that influence the overall rate and, hence, the productivity of the system were determined. To maximize the rate, the ferric:ferrous ion ratio and, hence, the biomass concentration, could be controlled by either reducing the reactor mean residence time or by applying external hydrodynamic stresses to the bioleach system.

In the following section, a dynamic analysis is performed on experimental data obtained from Raja.[20] Data relating to increased biological stress due to increased solids loading, defined as the mass of particles relative to the reactor volume [m/v], are presented. A dynamic analysis is then performed on a continuous flow system, applying the experimental data obtained from Raja[20] to show that the biomass and redox potential in a bioleach system can be effectively controlled at optimum conditions, using the analysis outlined in this study.

Experimental Validation

Raja[20] investigated the biological response of a *Sulfolobus metallicus* culture to hydrodynamic stress in a batch reactor at 341.15 K by increasing the solids loading. Inert quartzite particles, with a size fraction similar to the chalcopyrite concentrate 38×10^{-6} m to 75×10^{-6} m, were utilized in the experiments. Quartzite solids loading of 0, 6, 9 and 12% [m/v] were investigated for experiments containing 3% [m/v] chalcopyrite loading at a constant impeller tip speed. Raja[20] observed low-leaching rates throughout their experiments and attributed these low rates to high-initial solution potentials at which passivation was considered to occur. Raja[20] observed an increase in biological stress with an increase in solids loading, which resulted in a decrease in the redox potential, biomass concentration and, hence, the overall rate (Figure 11).

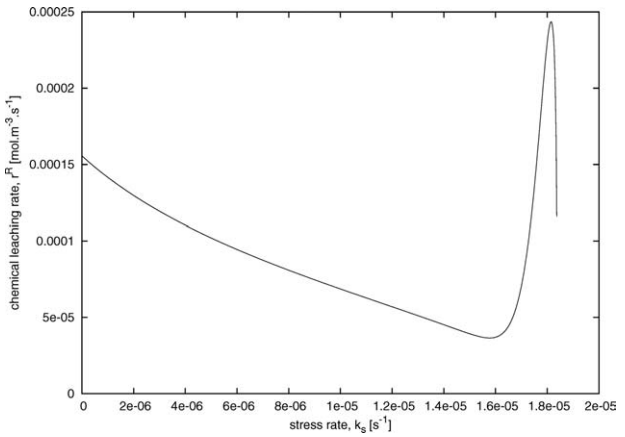

Figure 10. Comparison of the overall chemical leaching rate r^R achieved when no hydrodynamic stress is applied to the reactor system and when a stress rate of $k_s = 1.81 \times 10^{-5}$ s^{-1} is applied.

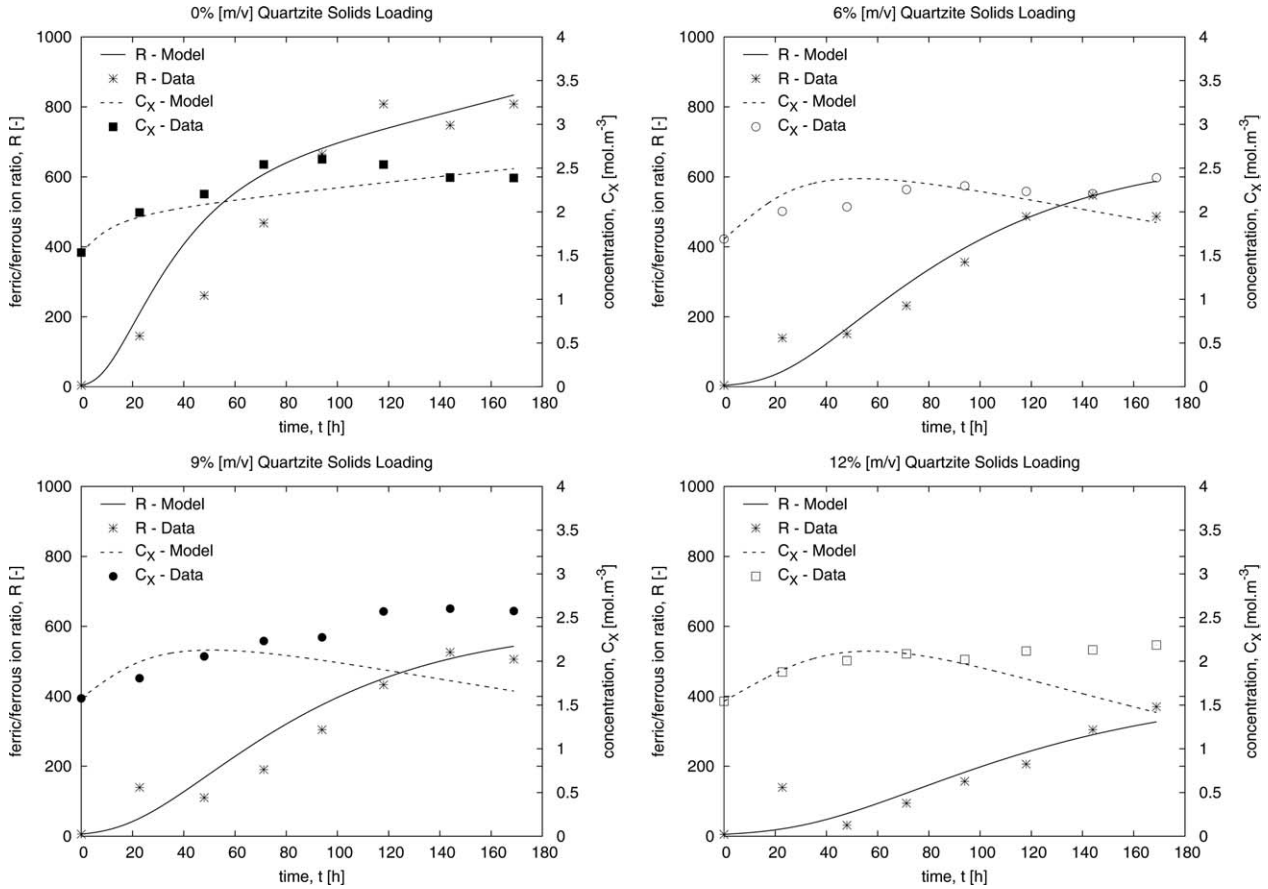

Figure 11. Model fit to batch ferric:ferrous ion ratio *R*, and biomass concentration C_X data obtained from Raja[20] for quartzite solids loadings ranging from 0–12% [m/v].

The results obtained from Raja[20] provide a framework for establishing an effective control system to maintain high leaching rates in a continuous flow system. Since the leaching rate constants A [mol m^{-2} s^{-1}] and B [mol m^{-2} s^{-1}], biomass yield Y_{XS} and biological stress rate k_s [s^{-1}] are unknown in these experiments, they were used as fitting parameters when validating the model with the experimental data. Microbial oxidation rate constants $q^{max}_{Fe^{2+}}$ for the *Sulfolobus metallicus* culture was assumed to correspond to the Arrhenius relationship established by Searby[22] and taken to equal 2.74×10^{-3} mol Fe^{2+} mol^{-1} carbon s^{-1} at 341.15 K with the inhibition constant $K = 0.019$.[22]

When fitting the data to the model, it was assumed that no biological stress was present in experiments with 0% [m/v] quartzite and 3% [m/v] chalcopyrite solids loading. Intrinsic leaching rate constants $A = 1.35 \times 10^{-6}$ mol m^{-2} s^{-1}, and

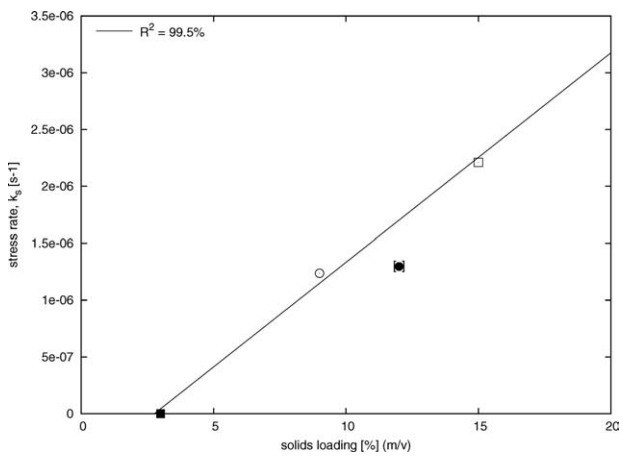

Figure 12. Resultant stress rates k_s obtained when 0–12% [m/v] quartzite solids loadings are applied to a batch reactor containing 3% [m/v] chalcopyrite concentrate.

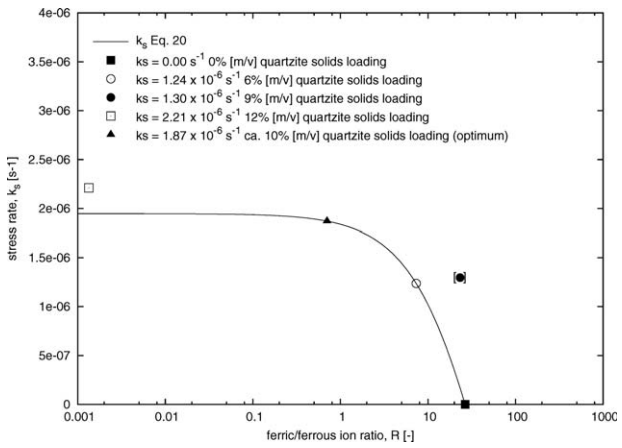

Figure 13. The biological stress rate as a function of ferric:ferrous ion ratio *R*.

Stress rates regressed from batch experiments performed by Raja[20] correspond well to the theoretical correlation outlined in Eq. 20.

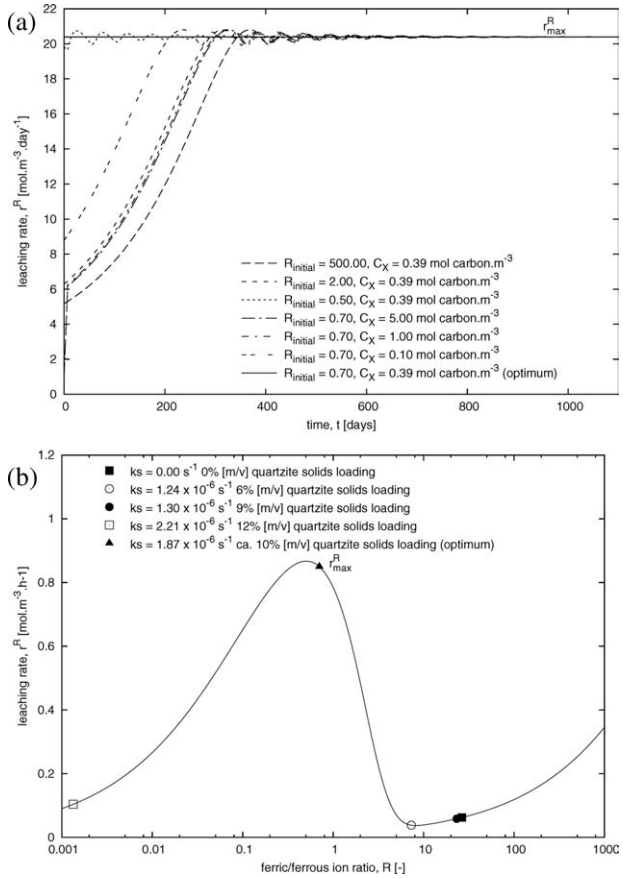

Figure 14. Overall leaching rate obtained in continuous flow system (a) and (b).

Maximum rates are achieved when a quartzite solids loading corresponding to ca. 10% [m/v] with a biological stress rate $k_s = 1.87 \times 10^{-6}$ s^{-1}, is applied.

$B = 5.67 \times 10^{-9}$ mol m^{-2} s^{-1} and biomass yield $Y_{XS} = 0.0021$ were found to best fit these data and, therefore, maintained constant in subsequent fits to experimental data containing 6, 9 and 12% [m/v] quartzite solids. The biological stress rate in experiments containing 6, 9 and 12% [m/v] quartzite solids was found to be 1.24×10^{-6}, 1.30×10^{-6} and 2.21×10^{-6} s^{-1}, respectively (Figure 11) and increased linearly with an increase in solids loading (Figure 12).

The kinetics constants obtained by fitting the batch data obtained from Raja[20] was applied to a dynamic analysis on a continuous flow system. To determine whether the batch data could be used in the continuous flow system, the biological stress rates k_s for the batch system were plotted with theoretical stress rates achieved for a continuous flow system operating at a mean residence time of 3 days using Eq. 1 (Figure 13). The model was able to predict the biological stress rates with reasonable accuracy and, therefore, reinforced the validity of a dynamic analysis on continuous flow system using the data obtained from Raja.[20]

Since the relationship between the solids loading and the resultant stress rate was established, an optimum stress rate to achieve high-leaching rates in the continuous system can be determined using the procedure outlined in the previous section. The dynamic analysis revealed that optimum leaching rates are achieved at $R_{X,max} = 0.70$ and $C_{X,max} = 0.39$ mol carbon m^{-3} Using Eq. 1, it was found that maximum rates could be achieved at the aforementioned conditions using a stress rate $k_s = 1.87 \times 10^{-6}$ s^{-1} (Figure 14). According to the experimental results obtained from Raja[20] and the relationship established in Figures 12 and 13 and Eq. 20, for biological stress rates resulting from increased solids loading in a bioleach reactor, about 10% [m/v] quartzite solids loading are required to maintain the system at optimum rates (Figure 14).

Figure 14a was generated by varying the reactor initial conditions. Two scenarios were considered. In the first case, the initial biomass concentration was maintained at the optimum $C_{X,max} = 0.39$ mol carbon m^{-3}, while the ferric:ferrous ion ratio was varied between 0.5–500. Thereafter the ferric:ferrous ion ratio was kept constant at the optimum operating point $R_{X,max} = 0.70$, while the biomass concentration was varied between 0.1–5.0 mol carbon m^{-3}. High rates r^R_{max} were obtained at about 10% [m/v] solids loading regardless of the reactor inlet conditions when the applied stress rate was kept at $k_s = 1.87 \times 10^{-6}$ s^{-1} (Figure 14).

Figure 14 verifies that, by applying a dynamic analysis to the bioleaching system, the system can be effectively driven to maintain the maximum rate r^R_{max} (Figure 14b). This rigorous approach to the dynamic analysis of chalcopyrite bioleaching shows that factors required to maintain high-bioleaching rates can be identified using the analysis presented in this study.

Conclusions

A nonmonotonic relationship between the intrinsic leaching rate of chalcopyrite with redox potential has been reported in literature, which, according to the dynamic analysis presented in this article, reveals that multiple steady states may exist during bioleaching. It is evident that as many as three steady states are possible in batch and continuous flow reactor systems. Stable steady states appear at low and high ferric:ferrous ion ratios with high- and low-bioleaching rates, respectively, with an unstable steady state at intermediate solution potentials. It was shown that the structure of the system dynamics was influenced by the biomass concentration, redox potential and mean residence time. Initial studies into the dynamics of chalcopyrite bioleaching were conducted using a fixed particle surface area assumption to determine the influence of the aforementioned operating modules. It was found that the system progresses from a single stable steady state at low ferric:ferrous ion ratios to multiple steady states and, thereafter, to a single stable steady state at high ferric:ferrous ion ratios with increasing biomass concentration, regardless of the reactor type.

A procedure for identifying the possible steady states for the bioleaching of mineral sulfide ores in continuous flow reactors was proposed. It was found that the continuous flow dynamics is composed of a batch term offset by a flow term. By increasing the mean residence time in a continuous flow reactor, the reactor operation approached batch operation.

A modified PBM was applied to the dynamic analysis to account for time-varying particle surface area. Results showed that the systems transitions from high-bioleaching rates at low-solution potentials to low rates at high ferric:ferrous ion ratios. Lower biomass concentrations were required to achieve these rates compared to batch and continuous flow reactors, which did not account for a change in particle surface area with time.

Two control procedures were proposed. Reducing the reactor mean residence time proved to be effective at maintaining high-bioleaching rates, whereas introducing an

external hydrodynamic stress rate to reduce the concentration of biomass in the system proved efficient at keeping the bioleaching system at both high rates and conversions. It was shown that in both interventions, a 56% increase over typical productivity could be achieved.

Application of the dynamic analysis to experimental data obtained from Raja[20] showed that the model was able to predict a solids loading that provides a biological stress rate that was able control the ferric:ferrous ion ratio and biomass concentrations at an optimum conditions to achieve maximum rates.

Notation

Greek letters

α = stoichiometric coefficient of the ferric ions in solution according the chemical leaching reaction
β = stoichiometric coefficient of the ferrous ions in solution according the chemical leaching reaction
θ = age of a particle, s
ϕ_{MS} = fraction of the pure mineral sulfide MS in the ore
τ = mean residence time, s

Latin symbols

A^P = particle specific surface area, $m^2\ kg^{-1}$
A^v = reactor-volume based particle specific surface area, $m^2\ m^{-3}$
A = temperature-dependent rate constant for the chemical leaching of chalcopyrite, mol $m^{-3}\ s^{-1}$
B = temperature-dependent rate constant for the chemical leaching of chalcopyrite, mol $m^{-3}\ s^{-1}$
C_{Fe3+} = concentration of ferric ions, mol m^{-3}
C_{Fe2+} = concentration of ferrous ions, mol m^{-3}
C_{MS} = concentration of mineral sulfide ore, mol m^{-3}
Cx = concentration of the biomass, mol carbon m^{-3}
$C_{X,a}$ = bifurcation biomass concentration at high ferric:ferrous ion ratios, mol carbon m^{-3}
$C_{X,b}$ = bifurcation biomass concentrations at low ferric:ferrous ion ratios, mol carbon m^{-3}
$C_{X,\max}$ = Biomass concentration required to maintain maximum overall rates, mol carbon m^{-3}
$f_0\ (l_0)$ = the normal distribution representing the probability of particles in a specific size range, m^{-1}
$f\ (X_{cpy})$ = topological term
g_{py} = mineral grade
$I\ (\theta)$ = the internal age distribution of particles, s^{-1}
K = inhibition constant
k_s = biological stress rate, s^{-1}
l_0 = initial particle size or diameter, m
M^P = mass of a particle, kg
N^T = the total number of particles in the reactor
$q^{max}_{Fe^{2+}}$ = the maximum microbial specific ferrous iron utilization rate, mol $Fe^{2+}\ mol^{-1}$ carbon s^{-1}
R = ferric:ferrous iron ratio, $R = [Fe^{3+}]/[Fe^{2+}]$
R_a = intercept point at high ferric:ferrous ion ratios
R_b = intercept point at low ferric:ferrous ion ratios
$R_{X,a}$ = ferric:ferrous ion ratio at bifurcation point $C_{X,a}$
$R_{X,b}$ = ferric:ferrous ion ratio at bifurcation point $C_{X,b}$
R_S = steady-state ferric:ferrous ion ratio
$R_{X,\max}$ = ferric/ferrous ion ratio required to maintain maximum overall rates
r'' = intrinsic surface reaction rate, mol $m^{-2}\ s^{-1}$
r_{cpy} = intrinsic chemical leaching rate for chalcopyrite, mol $m^{-2}\ s^{-1}$
$r_{Fe^{2+}_{ff}}$ = microbial oxidation rate, mol $m^{-3}\ s^{-1}$
r_{MS} = leaching rate of the mineral sulfide ore MS, mol $m^{-2}\ s^{-1}$
r^R = reactor bioleaching rate, mol $m^{-3}\ s^{-1}$
$r^R_{\max}$ = maximum reactor bioleaching rate, mol $m^{-3}\ s^{-1}$
t = time, s
V^R = reactor volume, m^3
X^R = overall reactor conversion
Y_{XS} = biomass yield

Literature Cited

1. Kotsiopoulos A, Hansford GS, Rawatlal R. An investigation into the dynamics of chalcopyrite bioleaching. *AIChE J*. 2010;56: 2650–2661.
2. Kotsiopoulos A, Hansford GS, Rawatlal R. An approach of segregation in modelling continuous flow tank bioleach systems. *AIChE J*. 2008;54:1592–1599.
3. Rawlings DE. Heavy metal mining using microbes. *Annu Rev Microbiol*. 2002;56:65–91.
4. Acevedo F. The use of reactors in biomining processes. *Electron J Biotechnol*. 2000;3:184–194.
5. Pinches A, Chapman JT, te Riele WAM, van Staden M. *The performance of bacterial leach reactors for the preoxidation of refactory gold bearing sulfide concentrates*. In: Norris PR, Kelly DP, editors. *Biohydrometallurgy, Proc. Int. Symp*. Warwick, STL, Kew, Surrey, UK; 1987:329–344.
6. Crundwell FK. Modeling, simulation and optimization of bacterial leaching reactors. *Biotechnol Bioeng*. 2001;71:257–265.
7. Crundwell FK. Mathematical modelling of batch and continuous bacterial leaching. *Chem Eng J*. 1994;54:207–220.
8. Crundwell FK. Progress in the mathematical modeling of leaching reactors. *Hydrometallurgy*. 1995;39:321–335.
9. Crundwell F. The leaching number: its definition and use in determining the performance of leaching reactors and autoclaves. *Minerals Eng*. 2005;18:1315–1324.
10. Breed AW, Hansford GS. Modeling continuous bioleach reactors. *Biotechnol Bioeng*. 1999;64:671–677.
11. Brochot S, Durance MV, Villeneuve J, d'Hugues P, Mugabi M. Modelling of the bioleaching of sulphide ores: Application for the simulation of the bioleaching/gravity section of the Kassese Cobalt Co., Ltd. process plant. *Minerals Eng*. 2004;17:253–260.
12. Rawatlal R and Starzak M. Unsteady-state residence-time distribution in perfectly mixed vessels. *AIChE J*. 2003;49:471–484.
13. Hansford GS, Miller DM. Biooxidation of a gold-bearing pyrite-arsenopyrite concentrate. *FEMS Microbiol Rev*. 1993;11:175–182.
14. Hansford GS. *Recent developments in modelling the kinetics of bioleaching*. In: Rawlings DE. *Biomining: Theory, Microbes and Industrial Processes*. Berlin, Germany: Springer; 1997:153–176.
15. Petersen J, Dixon DG. Competitive bioleaching of pyrite and chalcopyrite. *Hydrometallurgy*. 2006;83:40–49.
16. Hiroyoshi N, Kuroiwa S, Miki H, Tsunekawa M, Hirajima T. Synergistic effect of cupric and ferrous ions on active-passive behavior in anodic dissolution of chalcopyrite in sulfuric acid solutions. *Hydrometallurgy*. 2004;74:103–116.
17. Kametani H, Aoki A. Effect of suspension potential on the oxidation rate of copper concentrate in a sulphuric acid solution. *Metall Trans B*. 1985;16B:695–705.
18. Nemati M, Harrison STL. Effect of solid loading on thermophilic bioleaching of sulfide minerals. *J Chem Technol Biotechnol*. 2000;75:526–532.
19. Nemati M, Lowenadler J, Harrison STL. Particle size effects in bioleaching of pyrite by acidophilic thermophile *Sulfolobus metallicus* (BC). *Appl Microbiol Biotechnol*. 2000;53:173–179.
20. Raja SB. The Effect of Particulate-Induced Hydrodynamic Stress on the Bioleaching of Chalcopyrite by a Sulfolobus sp [Ph.D. thesis]. University of Cape Town, South Africa; 2005.
21. Valencia P, Acevedo F. Are bioleaching rates determined by the available particle surface area concentration? *World J Microbiol Biotechnol*. 2009;25:101–106.
22. Searby GE. An Investigation of the Kinetics of Thermophilic Microbial Ferrous Iron Oxidation in Continuous Culture [Ph.D. thesis]. University of Cape Town, South Africa; 2006.

Manuscript received Mar. 23, 2011, and revision received July 31, 2011.